

\mathcal{PT} -Symmetry Enhanced Berezinskii-Kosterlitz-Thouless Superfluidity

Yun-Mei Li, Xi-Wang Luo, and Chuanwei Zhang*

Department of Physics, The University of Texas at Dallas, Richardson, Texas 75080, USA

Berezinskii-Kosterlitz-Thouless (BKT) transition, the topological phase transition to a quasi-long range order in a two-dimensional (2D) system, is a hallmark of low-dimensional topological physics. The recent emergence of non-Hermitian physics, particularly parity-time (\mathcal{PT}) symmetry, raises a natural question about the fate of low-dimensional orders (e.g., BKT transition) in the presence of complex energy spectrum. Here we investigate the BKT phase transition in a 2D degenerate Fermi gas with an imaginary Zeeman field obeying \mathcal{PT} -symmetry. Despite complex energy spectrum, \mathcal{PT} -symmetry guarantees that the superfluid density and many other quantities are real. Surprisingly, the imaginary Zeeman field enhances the superfluid density, yielding higher BKT transition temperature than that in Hermitian systems. In the weak interaction region, the transition temperature can be much larger than that in the strong interaction limit. Our work showcases a surprising interplay between low-dimensional topological defects and non-Hermitian effects, paving the way for studying non-Hermitian low-dimensional phase transitions.

Berezinskii-Kosterlitz-Thouless (BKT) transition, first discovered in the two-dimensional (2D) XY spin model [1–4], is a cornerstone for studying low-dimensional condensed matter physics [5]. In 2D systems, while Mermin–Wagner theorem forbids the emergence of a true long range order due to thermal fluctuations, BKT physics permits a topological phase transition to a quasi-long range order of topological defects (i.e., vortices) at very low temperature. Specifically, across a critical temperature T_{BKT} , free vortices bind together spontaneously and form bound vortex-antivortex (V-AV) pairs, giving rising to a quasi-long range order. BKT transitions have been experimentally studied in a wide range of systems, including liquid helium films [6], 2D magnets [7–10], superconducting thin films [11–14], and 2D atomic hydrogen [15], where only macroscopic properties of the systems can be measured. In recent years, ultracold atomic superfluids have emerged as a versatile playground for the studies of BKT physics [16–29] with access to the underlying microscopic phenomena such as the visualization of the proliferation of free vortices. Experimental signatures of BKT physics have been observed in harmonically trapped Bose and Fermi gases [16–23], and the recent realization of ultracold superfluids in box potentials [30–34] offers a uniform platform for exploring BKT transitions.

So far the BKT transition has only been investigated in isolated systems governed by Hermitian Hamiltonians. The recent emergence of non-Hermitian physics, in particular parity-time (\mathcal{PT}) symmetry [35, 36], in photonic and ultracold atomic systems [37–43] raises a natural question on the fate of BKT transition in open systems, where the coupling with external environments leads to gain or loss that are generally described by non-Hermitian Hamiltonians. While the energy eigenvalues for non-Hermitian Hamiltonians are complex in general, the \mathcal{PT} -symmetry of a Hamiltonian ensures either all real (\mathcal{PT} -symmetric) or complex conjugate pairs (\mathcal{PT} -broken) of complex eigenvalues, with two regions

separated by an exceptional point [35, 36]. In ultracold atomic gases, the physical realization [40–43] as well as associated single particle physics [44–50] of \mathcal{PT} -symmetry have been investigated in both theory and experiment. Recently non-Hermitian fermionic superfluidity at zero temperature with complex-valued interactions or \mathcal{PT} -symmetric pairing states have been studied in theory [51–54]. However, non-Hermitian effects on the finite temperature BKT transitions in low-dimensional quantum systems remain unexplored.

In this Letter, we study the BKT phase transition in a 2D attractive Fermi gas in the presence of real in-plane and imaginary out-of-plane Zeeman fields that obey \mathcal{PT} -symmetry. In the \mathcal{PT} -symmetric region, quasi-particle eigenenergies are real and the BKT physics is similar as the Hermitian system. Interestingly, despite complex quasiparticle eigenenergies in the \mathcal{PT} -broken region, many physical quantities, such as order parameter and superfluid density are still real and oscillate with the imaginary Zeeman field. The superfluid density in the \mathcal{PT} -broken region is larger than that in the \mathcal{PT} -symmetric region, although the order parameter only changes slightly. As a result, the BKT temperature is higher in the \mathcal{PT} -broken region. In the weak coupling regime, the BKT transition temperature can be larger than the largest value $E_F/8$ for Hermitian system that is achieved in the strong coupling limit. The BKT transition temperature also shows an oscillating behavior with respect to the imaginary Zeeman field. Such surprising enhancement of BKT transition temperature showcases the interplay between non-Hermiticity and low-dimensional orders and phase transitions, which may open an avenue for exploring low-dimensional non-Hermitian physics.

Effective action: Consider a 2D degenerate Fermi gas with two atomic hyperfine states denoted as the pseudospin, where 2D confinement can be implemented by a strong harmonic trap or a deep optical lattice along the third dimension. The Fermi gas is subjected to real

in-plane (h_x) and imaginary out-of-plane (ih_z) Zeeman fields. The many-body Hamiltonian reads

$$H = \int d\mathbf{r} \hat{\Psi}^\dagger(\mathbf{r}) H_s(\mathbf{p}) \hat{\Psi}(\mathbf{r}) - U \int d\mathbf{r} \hat{\Psi}_\uparrow^\dagger(\mathbf{r}) \hat{\Psi}_\downarrow^\dagger(\mathbf{r}) \hat{\Psi}_\downarrow(\mathbf{r}) \hat{\Psi}_\uparrow(\mathbf{r}), \quad (1)$$

where the single-particle Hamiltonian $H_s(\mathbf{p}) = \mathbf{p}^2/2m - \mu + H_z$ with the chemical potential μ , Zeeman field $H_z = h_x \sigma_x + ih_z \sigma_z$ ($h_x, h_z > 0$), and Pauli matrices σ . $H_s(\mathbf{p})$ preserves a \mathcal{PT} -symmetry: $[H_s, \mathcal{PT}] = 0$ with $\mathcal{P} = \sigma_x$ and $\mathcal{T} = \mathcal{K}$, where \mathcal{K} denotes the complex conjugate. The exceptional point between \mathcal{PT} -symmetric and -broken regions is at $h_x = h_z$. U is the attractive interaction strength. $\hat{\Psi}(\mathbf{r}) = [\hat{\Psi}_\uparrow(\mathbf{r}), \hat{\Psi}_\downarrow(\mathbf{r})]^T$ and $\hat{\Psi}_\nu^\dagger(\mathbf{r})$ ($\hat{\Psi}_\nu(\mathbf{r})$) creates (annihilates) a fermionic atom at \mathbf{r} .

In quantum field theory, the partition function at temperature $T = 1/\beta$ can be written as a path integral $Z = \int D\bar{\phi} D\phi e^{-S_{\text{eff}}[\bar{\phi}, \phi]}$ with the effective action $S_{\text{eff}} = \int_0^\beta d\tau \int d\mathbf{r} \left[\frac{|\dot{\phi}|^2}{U} + \sum_{\mathbf{p}} \xi_{\mathbf{p}} \right] - \frac{1}{2} \text{Tr}[\ln G^{-1}]$, and $\xi_{\mathbf{p}} = \mathbf{p}^2/2m - \mu$. Here $\phi(\mathbf{r}, \tau)$ is the superfluid order parameter and the trace Tr is over momentum \mathbf{p} , imaginary time τ , and the Nambu index. The inverse Green function $G^{-1} = -\partial_\tau - H_{\text{BdG}}$, with the Bogoliubov-de Gennes (BdG) Hamiltonian in the Nambu basis given by

$$H_{\text{BdG}} = \begin{pmatrix} \xi_{\mathbf{p}} + ih_z & h_x & 0 & -\phi \\ h_x & \xi_{\mathbf{p}} - ih_z & \phi & 0 \\ 0 & \phi^* & -\xi_{\mathbf{p}} - ih_z & -h_x \\ -\phi^* & 0 & -h_x & -\xi_{\mathbf{p}} + ih_z \end{pmatrix}. \quad (2)$$

It is known that a large Zeeman field can induce finite-momentum Cooper pairing, *i.e.*, Fulde–Ferrell–Larkin–Ovchinnikov (FFLO) states [55, 56]. Here we are interested in the region with a small h_x . Assuming $\phi(\mathbf{r}, \tau) = \Delta e^{i\mathbf{q}\cdot\mathbf{r}}$ and using the mean-field saddle point $\frac{\partial S_{\text{eff}}}{\partial \Delta} = 0$, $\frac{\partial S_{\text{eff}}}{\partial \mathbf{q}} = 0$, we find that $\mathbf{q} = 0$ for a large imaginary field ih_z . Therefore we only consider zero momentum BCS pairing in this paper. The interaction parameter is regularized as $1/U = \sum_{\mathbf{k}} 1/(\hbar^2 k^2/m + E_B)$, where E_B is the two-body binding energy that can be varied by tuning the s -wave scattering length using Feshbach resonance or the barrier height along the z direction.

The quasiparticle spectrum has four branches $E = \pm E_{\mathbf{p}} \pm \sqrt{h_x^2 - h_z^2}$ with $E_{\mathbf{p}} = \sqrt{|\phi|^2 + \xi_{\mathbf{p}}^2}$, which are real (complex conjugate pairs) in the \mathcal{PT} -symmetric (-broken) region $h_z < h_x$ ($h_z > h_x$), as shown in Fig. 1. This property of the quasiparticle spectrum is guaranteed by the \mathcal{PT} -symmetry, which is still preserved for the BdG Hamiltonian with $\mathcal{P} = \sigma_x \tau_0$ and $\mathcal{T} = \mathcal{K}$. Here τ is the Pauli matrix on the particle-hole space. The BdG Hamiltonian also possesses a particle-hole symmetry $\mathcal{C} H_{\text{BdG}}(\mathbf{p}) \mathcal{C}^{-1} = -H_{\text{BdG}}^\dagger(-\mathbf{p})$ with $\mathcal{C} = \sigma_x \tau_y$ and $\mathcal{C}^2 = 1$. Due to the symmetry constraints, the effective

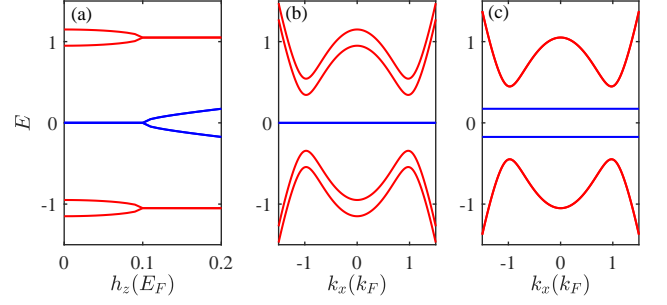


FIG. 1: (a) BdG quasiparticle energy spectrum with respect to h_z at $k_x = k_y = 0$. (b, c): Quasiparticle spectrum at $h_z = 0$ (b) and $h_z = 0.2E_F$ (c) along the k_x axis. $h_x = 0.1E_F$. Δ and μ are obtained self-consistently. The red and blue lines correspond to real and imaginary parts of the quasiparticle energies.

action at the saddle point

$$S_0 = \frac{\beta \Delta^2}{U} + \sum_{\mathbf{p}} [\beta \xi_{\mathbf{p}} - \ln(2 \cosh \beta h_{\text{eff}} + 2 \cosh \beta E_{\mathbf{p}})], \quad (3)$$

is always real even in the \mathcal{PT} -broken region, where $h_{\text{eff}} = \sqrt{h_x^2 - h_z^2}$. Similar result also applies to other quantities such as the partition function.

To study the phase fluctuations, we set $\phi(\mathbf{r}, \tau) = \Delta e^{i\theta(\mathbf{r}, \tau)}$, where $\theta(\mathbf{r}, \tau)$ is the phase fluctuation around the saddle point. Around the saddle point, the effective action can be written as $S_{\text{eff}} = S_0 + S_{\text{fluc}}$ with

$$S_{\text{fluc}} = \frac{1}{2} \int d^2\mathbf{r} [J(\nabla\theta)^2 + P(\partial_\tau\theta)^2 - Q(i\partial_\tau\theta)], \quad (4)$$

where

$$J = \frac{1}{4m} \sum_{\mathbf{p}} [n_{\mathbf{p}} - \frac{\beta \mathbf{p}^2}{8m} \sum_{i=\pm} \text{sech}^2 \frac{\beta E_i}{2}] \quad (5)$$

is the superfluid density, $P = \frac{1}{8} \sum_{\mathbf{p}} [\frac{\Delta^2}{E_{\mathbf{p}}^3} \sum_{i=\pm} \tanh \frac{\beta E_i}{2} + \frac{\beta \xi_{\mathbf{p}}^2}{2E_{\mathbf{p}}^2} \sum_{i=\pm} \text{sech}^2 \frac{\beta E_i}{2}]$ is the compressibility, $Q = \sum_{\mathbf{p}} n_{\mathbf{p}}$, $n_{\mathbf{p}} = 1 - \frac{\xi_{\mathbf{p}}}{2E_{\mathbf{p}}} \sum_{i=\pm} \tanh \frac{\beta E_i}{2}$, and $E_{\pm} = E_{\mathbf{p}} \pm h_{\text{eff}}$. In the \mathcal{PT} -broken region, the terms $\sum_{i=\pm} \tanh \frac{\beta E_i}{2} = \frac{2 \sinh(\beta E_{\mathbf{p}})}{\cosh(\beta E_{\mathbf{p}}) + \cos(\beta h')}$ in $n_{\mathbf{p}}$ and $\sum_{i=\pm} \text{sech}^2 \frac{\beta E_i}{2} = \frac{4[1 + \cosh(\beta E_{\mathbf{p}}) \cos(\beta h')]}{1 + 2 \cosh(\beta E_{\mathbf{p}}) \cos(\beta h') + [\cosh(2\beta E_{\mathbf{p}}) + \cos(2\beta h')]/2}$ [57] with real $h' = \sqrt{h_x^2 - h_z^2}$, therefore J is purely real as guaranteed by the \mathcal{PT} symmetry. In fact, the parameters J , P , Q are all real and positive, showing the superfluid phase is stable even in the \mathcal{PT} -broken region.

We can decompose the phase θ into a static vortex part $\theta_v(\mathbf{r})$ and a time-varying spin wave part $\theta_{sw}(\mathbf{r}, \tau)$, leading to $S_{\text{fluc}} = S_v + S_{sw}$ in the action of the phase fluctuation. Here $S_v = (1/2) \int d^2\mathbf{r} J(\nabla\theta_v)^2$,

$S_{sw} = (1/2) \int d^2\mathbf{r} [J(\nabla\theta_{sw})^2 + P(\partial_\tau\theta_{sw})^2 - Q(i\partial_\tau\theta_{sw})] = \sum_{\mathbf{k}} \ln[1 - \exp(-\beta\omega_{\mathbf{k}})]$, $\omega_{\mathbf{k}} = c|\mathbf{k}|$, and $c = \sqrt{J/P}$ is the sound speed. With the phase fluctuation, the parameters Δ and μ can be calculated self-consistently by solving the equations:

$$\frac{\partial S_0}{\partial \Delta} = 0, \quad \frac{\partial \Omega}{\partial \mu} = -n \quad (6)$$

with $\Omega = (S_0 + S_{sw})/\beta$ the thermodynamic potential. The atom density $n = mE_F/\pi$. $E_F = \hbar^2 k_F^2/2m$ and k_F^{-1} are chosen as the energy and length units, respectively. The mean-field transition temperature T_{MF} can be obtained from the saddle point equations with $\Delta = 0$, below which free vortices emerge ($\Delta \neq 0$) without phase coherence. The BKT phase transition temperature is determined self-consistently by [1–4]

$$T_{\text{BKT}} = \frac{\pi}{2} J(\Delta, \mu, T_{\text{BKT}}). \quad (7)$$

Across T_{BKT} , phase incoherent free vortices and anti-vortices transit to phase-coherent bound V-AV pairs, yielding a superfluid with a quasi-long range order. When the temperature further decreases below another critical temperature $T_{\text{vortex}} = 0.3J(\Delta, \mu, T_{\text{vortex}})$, V-AV pairs form a square lattice [58–60].

BKT transition with \mathcal{PT} symmetry: In Fig. 2 (a), we plot the superfluid density J with respect to h_z at a given $h_x = 0.1E_F$. In the \mathcal{PT} -symmetric region $h_z < h_x$, the single-particle Hamiltonian can be transformed to a Hermitian Hamiltonian $\hat{S}^{-1}(\xi_{\mathbf{p}} + h_x\sigma_x + ih_z\sigma_z)\hat{S} = \xi_{\mathbf{p}} + h_{\text{eff}}\sigma_x$, with $\hat{S} = e^{\alpha\sigma_y}$ and $\alpha = \frac{1}{4} \ln \frac{h_x - h_z}{h_x + h_z}$. Similarly, the transformation operator $\hat{S}' = e^{\alpha\sigma_y\tau_0}$ has the same effect on the BdG Hamiltonian (S13). It is known that the increase (decrease) of Zeeman field reduces (enhances) the order parameter in Hermitian systems, accompanied by the decrease (increase) of the superfluid density and the BKT transition temperature. Fig. 2 (a) shows that in the \mathcal{PT} -symmetric region the superfluid density increases as h_z increases, because the effective Zeeman field h_{eff} decreases. The 2D Fermi gas in the \mathcal{PT} -symmetric region behaves the same as a Hermitian system with a real Zeeman field.

In the \mathcal{PT} -broken region $h_z > h_x$, the quasiparticle spectrum is complex, but forms complex conjugate pairs due to the \mathcal{PT} symmetry (Fig. 1), which lead to real effective action and superfluid density. The superfluid density first increases, then oscillates with respect to h_z (Fig. 2 (a)) at fixed temperatures, which do not occur in BKT transitions for Hermitian systems. Such oscillation originates from the pair of complex conjugate quasiparticle eigenvalues, which lead to a periodic oscillation of

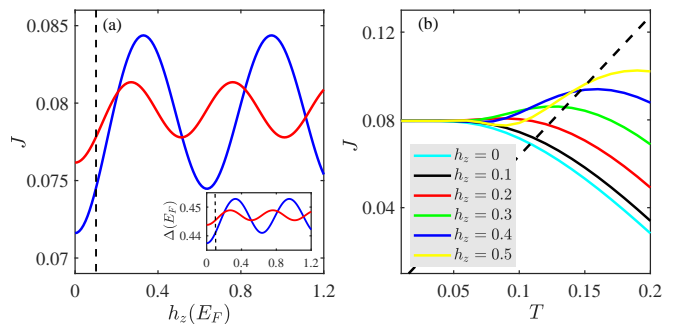


FIG. 2: The dependence of superfluid density J on h_z (a) and T (b). $E_b = 0.1E_F$, $h_x = 0.1E_F$. In (a), the blue and red lines denote the temperature $T = 0.1$ and 0.08 , respectively. The inset shows the order parameter Δ with respect to h_z . In (b), the intersection point between the black dashed line $y = 2T/\pi$ and superfluid density line corresponds to the BKT transition point.

the effective action at saddle point

$$S_0 = \frac{\beta\Delta^2}{U} + \sum_{\mathbf{p}} [\beta\xi_{\mathbf{p}} - \ln(2 \cos \beta h' + 2 \cosh \beta E_{\mathbf{p}})] \quad (8)$$

with the periodicity $\delta h' = 2\pi T$. Other parameters J , P , Q , Δ (inset in Fig. 2(a)), μ show a similar periodic dependence, as we see from the expression of J in the \mathcal{PT} -broken region (the paragraph below Eq. (5)). The oscillation amplitudes are smaller for lower temperatures, and the superfluid density in the \mathcal{PT} -broken region is larger than that in the \mathcal{PT} -symmetric region. The dependence of the superfluid density on the temperature is plotted in Fig. 2(b) for different h_z . At high temperature the superfluid density in the \mathcal{PT} -symmetric (-broken) region is smaller (larger) than that at the exceptional point $h_z = h_x$, which corresponds to the superfluid without Zeeman field.

From Eq. (7), the intersection points between J and the black dashed line $y = 2T/\pi$ in Fig. 2(b) correspond to the BKT transition points. Clearly, T_{BKT} is larger in the \mathcal{PT} -broken region. In Fig. 3(a), the dependence of T_{BKT} on the two-body binding energy E_B at different h_z is shown. The T_{BKT} in the \mathcal{PT} -broken region is always larger than that in the \mathcal{PT} -symmetric region for small binding energy and converges to $E_F/8$ in the strong coupling limit that is independent of the Zeeman fields. Surprisingly, in the \mathcal{PT} -broken region, T_{BKT} for weak coupling can be much larger than $E_F/8$, which was not discovered previously in Hermitian systems [24–28]. In both weak and strong coupling regions, the order parameter only changes slightly (Fig. 3 (b)). The unusual enlargement of T_{BKT} is determined by the non-Hermitian Zeeman field h_z , which enhances the fermionic superfluidity not through the order parameter.

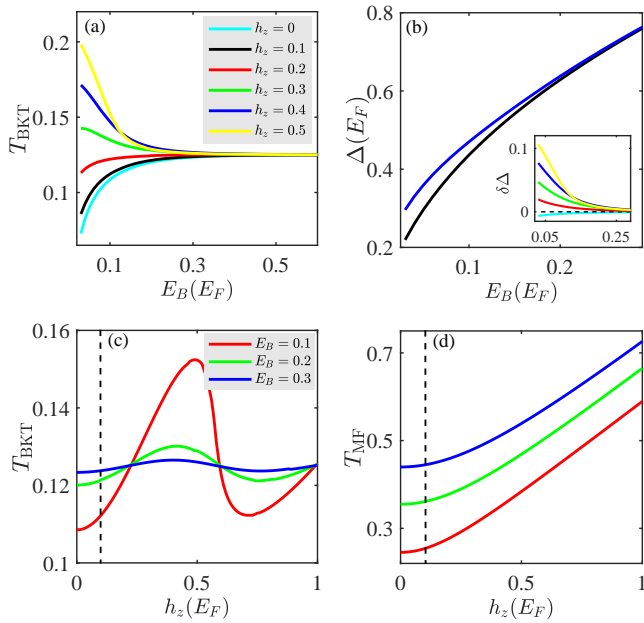


FIG. 3: (a) Dependence of T_{BKKT} on the binding energy E_B . (b) Dependence of the order parameter Δ at T_{BKKT} on E_B . The inset shows the Δ difference between $h_z = 0.1E_F$ and other h_z values. The color notation is the same as (a). (c,d) Dependence of T_{BKKT} (c) and mean-field temperature T_{MF} (d) on h_z . The black dashed line denotes the exceptional point. The line colors in (d) have the same notation as in (c). $h_x = 0.1E_F$ in all figures.

In the \mathcal{PT} -broken region, T_{BKKT} also oscillates with h_z around the equilibrium value $T_0 = E_F/8$ for a fixed E_B , as shown in Fig. 3(c). The oscillation amplitude is reduced for a large E_B . The oscillation period $\delta h' = 2\pi \times E_F/8 = \frac{\pi}{4}E_F$ is independent of E_B . In Fig. 3(d), we plot the mean-field temperature T_{MF} with respect to h_z , which increases as h_z or E_B increases. T_{MF} in the \mathcal{PT} -broken region is also larger than that in the symmetric region. However, T_{MF} does not show a periodic dependence on h_z in the \mathcal{PT} -broken region. Another critical temperature is the vortex lattice melting temperature T_{vortex} . T_{vortex} in the \mathcal{PT} -broken region is larger than that in \mathcal{PT} -symmetric region, and shows an oscillation with h_z but with a very small amplitude [57].

In Fig. 4, we plot the sound speed $c = \sqrt{J/P}$ with respect to T and h_z . Similar to the superfluid density, at high temperature, the sound speed in the \mathcal{PT} -broken region is always larger than that in the \mathcal{PT} -symmetric region. For a fixed binding energy E_B , the sound speed at T_{BKKT} oscillates with h_z with the period same as that for T_{BKKT} (Fig. 3(c)); while at a fixed temperature, the sound speed oscillates with h_z with the period same as that for superfluid density (Fig. 2(a)). The measurement of enhanced sound speed and its oscillation in the \mathcal{PT} -broken region can be used to detect the symmetry-

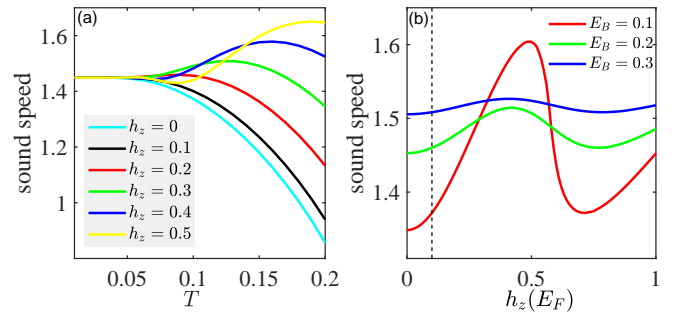


FIG. 4: Dependence of the sound speed on temperature T at different h_z in (a) and on h_z at T_{BKKT} in (b). $E_B = 0.1E_F$ in (a) and $h_x = 0.1E_F$ in both figures.

breaking physics [21, 61–64].

Discussion and summary: In the experimental realization of the \mathcal{PT} symmetric Hamiltonian, we can denote two atomic hyperfine states (e.g., $^2S_{1/2}, F = 1/2$ ground-state manifold of ^6Li) as the effective spin states. The real in-plane Zeeman field h_x can be realized using radio-frequency wave or microwave coupling. The imaginary Zeeman field can be achieved by introducing imbalanced loss to the two spins, which can be done by resonantly coupling the spin-down (or spin-up) state to the excited state using an optical beam. Usually, this process leads to an imaginary Zeeman field possessing \mathcal{PT} -symmetry (given by the loss rate difference between two spins) [41], together with some additional global loss term $-\frac{i\gamma_g}{2}\sigma_0$ (σ_0 2×2 is spin identity matrix). Fortunately, this term can be gauged out by a unitary transformation on inverse Green function G^{-1} with the operator $U' = e^{iM\gamma_g\tau/2}$ [57]. Effectively, this transformation replaces the order parameter ϕ with $\phi' = \phi e^{-i\gamma_g\tau}$ in Eq. (S13), which does not affect the action in Eq. (3) and superfluid parameters [57]. If we treat τ as the imaginary time, we see that ϕ' will decay at a rate γ_g as expected, indicating that we are discussing the instantaneous physics in a dissipative frame. This global loss would also lead to total atomic density decay, leading to the decay in energy and momentum units $E_F = n\pi/m$ and k_F (which means that the binding energy and Zeeman fields effectively increase with time). However, the enhancement of the instantaneous BKT transition temperature persists. Moreover, in realistic experiments, it is possible to couple the system with a reservoir (which can supply atoms or BCS pairs) to compensate the global atom loss instantaneously and thus maintain the atom density at some fixed value (*i.e.*, reaching equilibrium), yielding fixed BKT transition temperature.

In summary, we investigate the BKT phase transition in a non-Hermitian \mathcal{PT} symmetric 2D degenerate Fermi gas subject to an imaginary Zeeman field and find an enhanced BKT superfluidity with a very large BKT transi-

tion temperature at the weak coupling regime, in sharp contrast to the Hermitian system. Although we focus on the BKT physics with spin balanced atom density, it is possible to generalize the result to spin imbalanced [23, 56] or spin-orbit coupled 2D Fermi gases [65, 66], where non-Hermitian FFLO and/or topological states [67–69] may exist. Generalization to other BKT systems, such as Bose gases and 2D XY model could be another interesting direction. Our work showcases a surprising interplay between low-dimensional topological defects and non-Hermitian effects, paving the way for studying non-Hermitian low-dimensional phase transitions.

Acknowledgements: This work is supported by AFOSR (Grant No. FA9550-20-1-0220), NSF (Grant No. PHY-1806227), and ARO (Grant No. W911NF-17-1-0128).

* Electronic address: chuanwei.zhang@utdallas.edu

- [1] V. L. Berezinskii, Destruction of Long-range Order in One-dimensional and Two-dimensional Systems having a Continuous Symmetry Group. I. Classical Systems, *Sov. Phys. JETP* **32**, 493 (1971).
- [2] V. L. Berezinskii, Destruction of Long-range Order in One-dimensional and Two-dimensional Systems Possessing a Continuous Symmetry Group. II. Quantum Systems, *Sov. Phys. JETP* **34**, 610 (1971).
- [3] J. M. Kosterlitz and D. J. Thouless, Long range order and metastability in two dimensional solids and superfluids. (Application of dislocation theory), *J. Phys. C* **5**, L124 (1972).
- [4] J. M. Kosterlitz and D. J. Thouless, Ordering, metastability and phase transitions in two-dimensional systems, *J. Phys. C* **6**, 1181 (1973).
- [5] J. M. Kosterlitz, Nobel Lecture: Topological defects and phase transitions, *Rev. Mod. Phys.* **89**, 040501(2017).
- [6] D. J. Bishop and J. D. Reppy, Study of the Superfluid Transition in Two-Dimensional ^4He Films, *Phys. Rev. Lett.* **40**, 1727 (1978).
- [7] M. Heinrich, H.-A. K. von Nidda, A. Loidl, N. Rogado, and R. J. Cava, Potential Signature of a Kosterlitz-Thouless Transition in $\text{BaNi}_2\text{V}_2\text{O}_8$, *Phys. Rev. Lett.* **91**, 137601 (2003).
- [8] U. Tutsch, B. Wolf, S. Wessel, *et al.*, Evidence of a field-induced Berezinskii-Kosterlitz-Thouless scenario in a two-dimensional spin-dimer system, *Nature Commun.* **5**, 5169 (2014).
- [9] H. Li, Y. D. Liao, B.-B. Chen, X.-T. Zeng, X.-L. Sheng, Y. Qi, Z. Y. Meng, and W. Li, Kosterlitz-Thouless melting of magnetic order in the triangular quantum Ising material TmMgGaO_4 , *Nature Commun.* **11**, 1111 (2020).
- [10] Z. Hu, Z. Ma, Y.-D. Liao, *et al.*, Evidence of the Berezinskii-Kosterlitz-Thouless phase in a frustrated magnet, *Nature Commun.* **11**, 5631 (2020).
- [11] A. F. Hebard, A.T. Fiory, Evidence for the Kosterlitz-Thouless transition in thin superconducting aluminum films, *Phys. Rev. Lett.* **44**, 291 (1980).
- [12] K. Epstein, A. M. Goldman, and A. M. Kadin, Vortex-Antivortex Pair Dissociation in Two-Dimensional Superconductors, *Phys. Rev. Lett.* **47**, 534 (1981).
- [13] D. J. Resnick, J. C. Garland, J. T. Boyd, S. Shoemaker, and R. S. Newrock, Kosterlitz-Thouless Transition in Proximity-Coupled Superconducting Arrays, *Phys. Rev. Lett.* **47**, 1542 (1981).
- [14] M. Mondal, S. Kumar, M. Chand, A. Kamalpure, G. Saraswat, G. Seibold, L. Benfatto, and P. Raychaudhuri, Role of the Vortex-Core Energy on the Berezinskii-Kosterlitz-Thouless Transition in Thin Films of NbN, *Phys. Rev. Lett.* **107**, 217003 (2011).
- [15] A. I. Safonov, S. A. Vasilyev, I. S. Yasnikov, I. I. Lukashevich, and S. Jaakkola, Observation of Quasicondensate in Two-Dimensional Atomic Hydrogen, *Phys. Rev. Lett.* **81**, 4545 (1998).
- [16] Z. Hadzibabic, P. Krüger, M. Cheneau, B. Battelier, and Jean Dalibard, Berezinskii-Kosterlitz-Thouless crossover in a trapped atomic gas, *Nature (London)* **441**, 1118 (2006).
- [17] R. Desbuquois, L. Chomaz, T. Yefsah, J. Leonard, J. Beugnon, C. Weitenberg, and J. Dalibard, Superfluid behaviour of a two-dimensional Bose gas, *Nat. Phys.* **8**, 645 (2012).
- [18] P. Clade, C. Ryu, A. Ramanathan, K. Helmereson, and W. D. Phillips, Observation of a 2D Bose gas: From thermal to quasicondensate to superfluid. *Phys. Rev. Lett.* **102**, 170401 (2009).
- [19] S. Tung, G. Lamporesi, D. Lobser, L. Xia, and E. A. Cornell, Observation of the presuperfluid regime in a two-dimensional Bose gas. *Phys. Rev. Lett.* **105**, 230408 (2010).
- [20] P. A. Murthy, I. Boettcher, L. Bayha, M. Holzmann, D. Kedar, M. Neidig, M. G. Ries, A. N. Wenz, G. Zurn, and S. Jochim, Observation of the Berezinskii-Kosterlitz-Thouless Phase Transition in an Ultracold Fermi Gas, *Phys. Rev. Lett.* **115**, 010401 (2015).
- [21] P. Christodoulou, M. Gałka, N. Dogra, R. Lopes, J. Schmitt, and Z. Hadzibabic, Observation of first and second sound in a BKT superfluid, *Nature* **594**, 191 (2021).
- [22] L. Sobirey, N. Luick, M. Bohlen, H. Biss, H. Moritz, and T. Lompe, Observation of superfluidity in a strongly correlated two-dimensional Fermi gas, *Science* **372**, 844 (2021).
- [23] D. Mitra, P. T. Brown, P. Schauß, S. S. Kondov, and W. S. Bakr, Phase Separation and Pair Condensation in a Spin-Imbalanced 2D Fermi Gas, *Phys. Rev. Lett.* **117**, 093601 (2016).
- [24] S. S. Botelho and C. A. R. Sá de Melo, Vortex-Antivortex Lattice in Ultracold Fermionic Gases, *Phys. Rev. Lett.* **96**, 040404 (2006).
- [25] G. Bertaina and S. Giorgini, BCS-BEC Crossover in a Two-Dimensional Fermi Gas, *Phys. Rev. Lett.* **106**, 110403 (2011).
- [26] M. Gong, G. Chen, S. Jia, and C. Zhang, Searching for Majorana Fermions in 2D Spin-Orbit Coupled Fermi Superfluids at Finite Temperature, *Phys. Rev. Lett.* **109**, 105302 (2012).
- [27] J. P. A. Devreese, J. Tempere, and C. A. R. Sá de Melo, Effects of Spin-Orbit Coupling on the Berezinskii-Kosterlitz-Thouless Transition and the Vortex-Antivortex Structure in Two-Dimensional Fermi Gases, *Phys. Rev. Lett.* **113**, 165304 (2014).
- [28] Y. Xu and C. Zhang, Berezinskii-Kosterlitz-Thouless Phase Transition in 2D Spin-Orbit-Coupled Fulde-Ferrell Superfluids, *Phys. Rev. Lett.* **114**, 110401 (2015).

- [29] C.-T. Wu, B. M. Anderson, R. Boyack, and K. Levin, Quasicondensation in Two-Dimensional Fermi Gases, *Phys. Rev. Lett.* **115**, 240401 (2015).
- [30] C.-S. Chuu, J. Hanssen, F. Schreck, and M. G. Raizen, Bose-Einstein Condensate in a Box, *Phys. Rev. A* **71**, 041604 (2005).
- [31] A. L. Gaunt, T. F. Schmidutz, I. Gotlibovych, R. P. Smith, and Z. Hadzibabic, Bose-Einstein Condensation of Atoms in a Uniform Potential, *Phys. Rev. Lett.* **110**, 200406 (2013).
- [32] B. Mukherjee, Z. Yan, P. B. Patel, Z. Hadzibabic, T. Yefsah, J. Struck, and M. W. Zwierlein, Homogeneous Atomic Fermi Gases, *Phys. Rev. Lett.* **118**, 123401 (2017).
- [33] K. Hueck, N. Luick, L. Sobirey, J. Siegl, T. Lompe, and H. Moritz, Two-Dimensional Homogeneous Fermi Gases, *Phys. Rev. Lett.* **120**, 060402 (2018).
- [34] P. B. Patel, Z. Yan, B. Mukherjee, R. J. Fletcher, J. Struck, and M. W. Zwierlein, Universal sound diffusion in a strongly interacting Fermi gas, *Science* **370**, 1222 (2020).
- [35] C. M. Bender and S. Boettcher, Real Spectra in Non-Hermitian Hamiltonians Having \mathcal{PT} Symmetry, *Phys. Rev. Lett.* **80**, 5243 (1998).
- [36] C. M. Bender, Making sense of non-Hermitian Hamiltonians, *Rep. Prog. Phys.* **70**, 947 (2007).
- [37] R. El-Ganainy, K. G. Makris, M. Khajavikhan, Z. H. Musslimani, S. Rotter, and D. N. Christodoulides, Non-Hermitian physics and \mathcal{PT} symmetry, *Nat. Phys.* **14**, 11 (2018).
- [38] L. Feng, R. El-Ganainy and L. Ge, Non-Hermitian photonics based on parity-time symmetry, *Nature Photonics* **11**, 752 (2017).
- [39] M. Müller, S. Diehl, G. Pupillo, and P. Zoller, Engineered open systems and quantum simulations with atoms and ions, *Adv. At. Mol. Opt. Phys.* **61**, 1 (2012).
- [40] P. Peng, W. Cao, C. Shen, W. Qu, J. Wen, L. Jiang and Y. Xiao, Anti-parity-time symmetry with flying atoms, *Nature Phys.* **12**, 1139(2016).
- [41] J. Li, A. K. Harter, J. Liu, L. de Melo, Y. N. Joglekar, and L. Luo, Observation of parity-time symmetry breaking transitions in a dissipative Floquet system of ultracold atoms, *Nat. Commun.* **10**, 855 (2019).
- [42] S. Lapp, J. Ang'ong'a, F. A. An and B. Gadway, Engineering tunable local loss in a synthetic lattice of momentum states, *New J. Phys.* **21** 045006 (2019).
- [43] Y. Takasu, T. Yagami, Y. Ashida, R. Hamazaki, Y. Kuno, Y. Takahashi, \mathcal{PT} -symmetric non-Hermitian quantum many-body system using ultracold atoms in an optical lattice with controlled dissipation, *Prog. Theor. Exp. Phys.* **2020**, 12A110 (2020).
- [44] Y. Ashida, S. Furukawa, and M. Ueda, Parity-time-symmetric quantum critical phenomena, *Nature Commun.* **8**, 15791 (2017).
- [45] X.-W. Luo and C. Zhang, Higher-Order Topological Corner States Induced by Gain and Loss, *Phys. Rev. Lett.* **123**, 073601 (2019).
- [46] T. Yoshida, R. Peters, and N. Kawakami, Non-Hermitian perspective of the band structure in heavy-fermion systems, *Phys. Rev. B* **98**, 035141 (2018).
- [47] Y. Xu, S.-T. Wang, and L.-M. Duan, Weyl Exceptional Rings in a Three-Dimensional Dissipative Cold Atomic Gas, *Phys. Rev. Lett.* **118**, 045701 (2017).
- [48] L. Li, C. H. Lee, and J. Gong, Topological Switch for Non-Hermitian Skin Effect in Cold-Atom Systems with Loss, *Phys. Rev. Lett.* **124**, 250402 (2020).
- [49] J. Xu, Y.-X. Du, W. Huang, and D.-W. Zhang, Detecting topological exceptional points in a parity-time symmetric system with cold atoms, *Optics Express* **25**, 15786 (2017).
- [50] T. Liu, Y.-R. Zhang, Q. Ai, Z. Gong, K. Kawabata, M. Ueda, and F. Nori, Second-Order Topological Phases in Non-Hermitian Systems, *Phys. Rev. Lett.* **122**, 076801 (2019).
- [51] N. M. Chtchelkatchev, A. A. Golubov, T. I. Baturina, and V. M. Vinokur, Stimulation of the Fluctuation Superconductivity by \mathcal{PT} Symmetry, *Phys. Rev. Lett.* **109**, 150405 (2012).
- [52] A. Ghatak and T. Das, Theory of superconductivity with non-Hermitian and parity-time reversal symmetric Cooper pairing symmetry, *Phys. Rev. B* **97**, 014512 (2018).
- [53] L. Zhou, X. Cui, Enhanced Fermion Pairing and Superfluidity by an Imaginary Magnetic Field, *iScience* **14**, 257 (2019).
- [54] K. Yamamoto, M. Nakagawa, K. Adachi, K. Takasan, M. Ueda, and N. Kawakami, Theory of Non-Hermitian Fermionic Superfluidity with a Complex-Valued Interaction, *Phys. Rev. Lett.* **123**, 123601 (2019).
- [55] Y. A. Liao, A. S. C. Rittner, T. Paprotta, W. Li, G. B. Partridge, R. G. Hulet, S. K. Baur, and E. J. Mueller, Spin-imbalance in a one-dimensional Fermi gas, *Nature* **467**, 567 (2010).
- [56] W. Ong, Chingyun Cheng, I. Arakelyan, and J. E. Thomas, Spin-Imbalanced Quasi-Two-Dimensional Fermi Gases, *Phys. Rev. Lett.* **114**, 110403 (2015).
- [57] See SupplementalMaterial for details of our calculation and derivation.
- [58] B. I. Halperin and D. R. Nelson, Theory of Two-Dimensional Melting, *Phys. Rev. Lett.* **41**, 121 (1978).
- [59] D. R. Nelson and B. I. Halperin, Dislocation-mediated melting in two dimensions, *Phys. Rev. B* **19**, 2457 (1979).
- [60] A. P. Young, Melting and the vector Coulomb gas in two dimensions, *Phys. Rev. B* **19**, 1855 (1979).
- [61] L. A. Sidorenkov, M. K. Tey, R. Grimm, Y.-H. Hou, L. Pitaevskii, and S. Stringari, Second sound and the superfluid fraction in a Fermi gas with resonant interactions, *Nature* **498**, 78 (2013).
- [62] L. Salasnich, P. A. Marchetti, and F. Toigo, Superfluidity, sound velocity, and quasicondensation in the two-dimensional BCS-BEC crossover, *Phys. Rev. A* **88**, 053612 (2013).
- [63] T. Ozawa and S. Stringari, Discontinuities in the First and Second Sound Velocities at the Berezinskii-Kosterlitz-Thouless Transition, *Phys. Rev. Lett.* **112**, 025302 (2014).
- [64] M. Bohlen, L. Sobirey, N. Luick, H. Biss, T. Enss, T. Lompe, and H. Moritz, Sound Propagation and Quantum-Limited Damping in a Two-Dimensional Fermi Gas, *Phys. Rev. Lett.* **124**, 240403 (2020).
- [65] Y.-J. Lin, K. Jiménez-García, and I. B. Spielman, Spin-orbit-coupled Bose-Einstein condensates, *Nature (London)* **471**, 83 (2011).
- [66] P. Wang, Z.-Q. Yu, Z. Fu, J. Miao, L. Huang, S. Chai, H. Zhai, and J. Zhang, Spin-Orbit Coupled Degenerate Fermi Gases, *Phys. Rev. Lett.* **109**, 095301 (2012).
- [67] C. Zhang, S. Tewari, Roman M. Lutchyn, and

- S. Das Sarma, $p_x + ip_y$ Superfluid from s-Wave Interactions of Fermionic Cold Atoms, *Phys. Rev. Lett.* **101**, 160401 (2008).
- [68] W. Zhang, and W. Yi, Topological Fulde-Ferrell-Larkin-Ovchinnikov states in spin-orbit-coupled Fermi gases, *Nat. Commun.* **4**, 2711 (2013).

- [69] C. Qu, Z. Zheng, M. Gong, Y. Xu, L. Mao, X. Zou, G. Guo, and C. Zhang, Topological superfluids with finite-momentum pairing and Majorana fermions, *Nat. Commun.*, **4**, 2710 (2013).

SUPPLEMENTARY MATERIALS

S1. Real physical quantities in \mathcal{PT} -broken phase

From the main text, the effective action at the saddle point after integrating out the Fermi fields is given by

$$S_{\text{eff}} = \beta \left(\frac{|\phi|^2}{U} + \sum_{\mathbf{p}} \xi_{\mathbf{p}} \right) - \frac{1}{2} \text{Tr}[\ln G^{-1}], \quad (\text{S1})$$

with the inverse Green function $G^{-1} = -\partial_{\tau} - H_B$. Replacing ∂_{τ} with $-i\omega_n$, we get

$$S_{\text{eff}} = \beta \left(\frac{|\phi|^2}{U} + \sum_{\mathbf{p}} \xi_{\mathbf{p}} \right) - \frac{1}{2} \sum_{n, \mathbf{p}} \ln \left\{ \prod_{\pm} [(i\omega_n - E_{\pm})(i\omega_n + E_{\pm})] \right\}, \quad (\text{S2})$$

where $\omega_n = \frac{(2n+1)\pi}{\beta}$ and $E_{\pm} = \sqrt{\xi_{\mathbf{p}}^2 + |\phi|^2} \pm \sqrt{h_x^2 - h_z^2}$. The eigenvalues E_{\pm} always locate at the right half-plane in the complex plane. After summation over the Matsubara frequency,

$$S_{\text{eff}} = \beta \left(\frac{|\phi|^2}{U} + \sum_{\mathbf{p}} \xi_{\mathbf{p}} \right) - \sum_{\mathbf{p}} \{ \ln[1 + e^{-2\beta E_{\mathbf{p}}} + 2e^{-\beta E_{\mathbf{p}}} \cosh(\beta h_{\text{eff}})] + \beta E_{\mathbf{p}} \} \quad (\text{S3})$$

$E_{\mathbf{p}} = \sqrt{\xi_{\mathbf{p}}^2 + |\phi|^2}$, $h_{\text{eff}} = \sqrt{h_x^2 - h_z^2}$. In the \mathcal{PT} -symmetric region, $h_x > h_z$, the effective action is real. In the \mathcal{PT} -broken region, $h_x < h_z$, $h_{\text{eff}} = ih'$ with $h' = \sqrt{h_z^2 - h_x^2}$, and the effective action becomes

$$S_{\text{eff}} = \beta \left(\frac{|\phi|^2}{U} + \sum_{\mathbf{p}} \xi_{\mathbf{p}} \right) - \sum_{\mathbf{p}} \{ \ln[1 + e^{-2\beta E_{\mathbf{p}}} + 2e^{-\beta E_{\mathbf{p}}} \cos(\beta h')] + \beta E_{\mathbf{p}} \}. \quad (\text{S4})$$

The term inside the logarithmic function is always larger than 0, and the effective action at the saddle point in the \mathcal{PT} -broken region is also real. As a result, the partition function is real and positive.

Now we prove the superfluid parameters J , P , Q are real in the \mathcal{PT} -broken region. They are given by

$$J = \frac{1}{4m} \sum_{\mathbf{p}} \left[n_{\mathbf{p}} - \frac{\beta \mathbf{p}^2}{8m} \sum_{i=\pm} \text{sech}^2 \frac{\beta E_i}{2} \right], \quad (\text{S5})$$

$$P = \frac{1}{8} \sum_{\mathbf{p}} \left[\frac{\Delta^2}{E_{\mathbf{p}}^3} \sum_{i=\pm} \tanh \frac{\beta E_i}{2} + \frac{\beta \xi_{\mathbf{p}}^2}{2E_{\mathbf{p}}^2} \sum_{i=\pm} \text{sech}^2 \frac{\beta E_i}{2} \right], \quad (\text{S6})$$

$$Q = \sum_{\mathbf{p}} n_{\mathbf{p}}, \quad n_{\mathbf{p}} = 1 - \frac{\xi_{\mathbf{p}}}{2E_{\mathbf{p}}} \sum_{i=\pm} \tanh \frac{\beta E_i}{2} \quad (\text{S7})$$

From the expressions, we only need prove two terms $\sum_{i=\pm} \tanh \frac{\beta E_i}{2}$ and $\sum_{i=\pm} \text{sech}^2 \frac{\beta E_i}{2}$ are real. For the first term

$$\begin{aligned} \sum_{i=\pm} \tanh \frac{\beta E_i}{2} &= \tanh \frac{\beta(E_+ + E_-)}{2} \left(1 + \tanh \frac{\beta E_+}{2} \tanh \frac{\beta E_-}{2}\right) \\ &= \tanh(\beta E_{\mathbf{p}}) \left(1 + \frac{\sinh \frac{\beta E_+}{2} \sinh \frac{\beta E_-}{2}}{\cosh \frac{\beta E_+}{2} \cosh \frac{\beta E_-}{2}}\right) \\ &= \tanh(\beta E_{\mathbf{p}}) \left[1 + \frac{\cosh(\beta E_{\mathbf{p}}) - \cosh(\beta h_{\text{eff}})}{\cosh(\beta E_{\mathbf{p}}) + \cosh(\beta h_{\text{eff}})}\right]. \end{aligned} \quad (\text{S8})$$

In the \mathcal{PT} -broken region, $\cosh(\beta h_{\text{eff}}) = \cos(\beta h')$, and we obtain

$$\sum_{i=\pm} \tanh \frac{\beta E_i}{2} = \frac{2 \sinh(\beta E_{\mathbf{p}})}{\cosh(\beta E_{\mathbf{p}}) + \cos(\beta h')}, \quad (\text{S9})$$

which is real. For the second term,

$$\begin{aligned} \sum_{i=\pm} \text{sech}^2 \frac{\beta E_i}{2} &= \frac{2}{1 + \cosh(\beta E_+)} + \frac{2}{1 + \cosh(\beta E_-)} \\ &= \frac{4 + 2 \cosh(\beta E_+) + 2 \cosh(\beta E_-)}{1 + \cosh(\beta E_+) + \cosh(\beta E_-) + \cosh(\beta E_+) \cosh(\beta E_-)} \\ &= \frac{4 + 4 \cosh(\beta E_{\mathbf{p}}) \cosh(\beta h_{\text{eff}})}{1 + 2 \cosh(\beta E_{\mathbf{p}}) \cosh(\beta h_{\text{eff}}) + [\cosh(2\beta E_{\mathbf{p}}) + \cosh(2\beta h_{\text{eff}})]/2}. \end{aligned} \quad (\text{S10})$$

In the \mathcal{PT} -broken region, we obtain

$$\sum_{i=\pm} \text{sech}^2 \frac{\beta E_i}{2} = \frac{4 [1 + \cosh(\beta E_{\mathbf{p}}) \cos(\beta h')]}{1 + 2 \cosh(\beta E_{\mathbf{p}}) \cos(\beta h') + [\cosh(2\beta E_{\mathbf{p}}) + \cos(2\beta h')]/2}, \quad (\text{S11})$$

which is also real.

S2. Lattice melting temperature T_{vortex}

In Fig. S1, we plot the vortex lattice melting temperature T_v with respect to the binding energy E_B and imaginary Zeeman field h_z . Similar as T_{BKT} , T_{vortex} in the \mathcal{PT} -broken region is larger at the weak coupling regime and then converges to the value $\frac{3E_F}{40\pi} \approx 0.0239E_F$ at the strong coupling limit. T_{vortex} in the \mathcal{PT} -broken region can be larger than the strong coupling limit value. In (b), we see T_{vortex} also shows an oscillating behavior for a given E_B with the equilibrium center $\frac{3E_F}{40\pi}$ in the \mathcal{PT} -broken region. The oscillation period is $\delta h' = 2\pi \times \frac{3E_F}{40\pi} = \frac{3E_F}{20}$ and the oscillation amplitude of T_{vortex} is quite small.

S4. BKT PHYSICS WITH IMBALANCED GAIN AND LOSS

An exact \mathcal{PT} -symmetric Hamiltonian is usually hard to realize. For example, a global loss term $-i\gamma\sigma_0$ on both spin species will break the \mathcal{PT} symmetry in the single-particle Hamiltonian $H_s(\mathbf{p}) = \xi_{\mathbf{p}} + h_x\sigma_x + ih_z\sigma_z - i\gamma\sigma_0$. Then the partition function $Z = \int D\bar{\phi}D\phi e^{-S_{\text{eff}}[\bar{\phi},\phi]}$ with the effective action $S_{\text{eff}} = \int_0^\beta d\tau \int d\mathbf{r} \left(\frac{|\dot{\phi}|^2}{U} + \sum_{\mathbf{p}} (\xi_{\mathbf{p}} - i\gamma)\right) - \frac{1}{2} \text{Tr}[\ln G^{-1}]$. The inverse Green function $G^{-1} = -\partial_\tau - H_{\text{BdG}}$, where the BdG Hamiltonian in the Nambu basis is given by

$$H_{\text{BdG}} = \begin{pmatrix} H_s(\mathbf{p}) & -i\phi\sigma_y \\ i\phi^*\sigma_y & -H_s(-\mathbf{p}) \end{pmatrix}. \quad (\text{S12})$$

We can introduce a transformation $U^{-1}G^{-1}U$ with $U = \exp(iM\gamma\tau)$ and $M = \text{diag}(1, 1, -1, -1)$ to gauge out the diagonal γ terms. The effective action becomes $S_{\text{eff}} = \int_0^\beta d\tau \int d\mathbf{r} \left(\frac{|\dot{\phi}|^2}{U} + \sum_{\mathbf{p}} \xi_{\mathbf{p}}\right) - \frac{1}{2} \text{Tr}[\ln(G^{-1})']$ with $(G^{-1})' =$

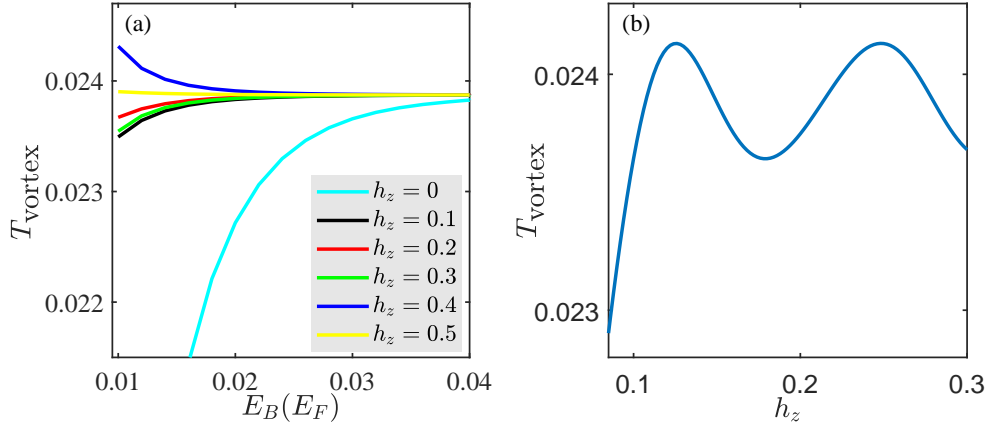


FIG. S1: The vortex melting temperature versus E_B (a) and h_z (b), respectively. In (b), $E_B = 0.012E_F$. In (a) and (b), $h_x = 0.1E_F$.

$-\partial_\tau - H'_{\text{BdG}}$ and

$$H'_{\text{BdG}} = \begin{pmatrix} \xi_{\mathbf{p}} + ih_z & h_x & 0 & -\phi' \\ h_x & \xi_{\mathbf{p}} - ih_z & \phi' & 0 \\ 0 & \phi'^* & -\xi_{\mathbf{p}} - ih_z & -h_x \\ -\phi'^* & 0 & -h_x & -\xi_{\mathbf{p}} + ih_z \end{pmatrix}. \quad (\text{S13})$$

with $\phi' = \phi e^{-2i\gamma\tau}$. The Nambu basis is now $\Psi = (e^{-i\gamma\tau}\Psi_{\mathbf{p}\uparrow}, e^{-i\gamma\tau}\Psi_{\mathbf{p}\downarrow}, e^{i\gamma\tau}\Psi_{-\mathbf{p}\downarrow}^\dagger, e^{i\gamma\tau}\Psi_{-\mathbf{p}\uparrow}^\dagger)^T$. This means we can construct a \mathcal{PT} -symmetric system in the dissipative frame since τ is the imaginary time. In this transformation, $\phi\phi^* = \phi'\phi'^*$. As a result, the effective action in Eq. (3) and the superfluid parameters in the main text will stay the same. Notice that the \mathcal{PT} -symmetric non-Hermitian term $ih_z\sigma_z$ cannot be gauged out by the above method.